J Physiol (2003), **546.3**, *pp.* 801–811
DOI: 10.1113/jphysiol.2002.032730

www.jphysiol.org

Journal of Physiology

Strong, reliable and precise synaptic connections between thalamic relay cells and neurones of the nucleus reticularis in juvenile rats

Luc J. Gentet and Daniel Ulrich

Institute of Physiology, University of Bern, Bühlplatz 5, 3012 Bern, Switzerland

The thalamic reticular nucleus (nRT) is composed entirely of GABAergic inhibitory neurones that receive input from pyramidal cortical neurones and excitatory relay cells of the ventrobasal complex of the thalamus (VB). It plays a major role in the synchrony of thalamic networks, yet the synaptic connections it receives from VB cells have never been fully physiologically characterised. Here, whole-cell current-clamp recordings were obtained from 22 synaptically connected VB–nRT cell pairs in slices of juvenile (P14–20) rats. At 34–36 °C, single presynaptic APs evoked unitary EPSPs in nRT cells with a peak amplitude of 7.4 ± 1.5 mV (mean ± S.E.M.) and a decay time constant of 15.1 ± 0.9 ms. Only four out of 22 pairs showed transmission failures at a mean rate of 6.8 ± 1.1 %. An NMDA receptor (NMDAR)-mediated component was significant at rest and subsequent EPSPs in a train were depressed. Only one out of 14 pairs tested was reciprocally connected; the observed IPSPs in the VB cell had a peak amplitude of 0.8 mV and were completely abolished in the presence of 10 μM bicuculline. Thus, synaptic connections from VB cells to nRT neurones are mainly 'drivers', while a small subset of cells form closed disynaptic loops.

(Received 19 September 2002; accepted after revision 11 November 2002; first published online 13 December 2002)
Corresponding author L. J. Gentet: Institute of Physiology, University of Bern, Bühlplatz 5, 3012 Bern, Switzerland.
Email: gentet@pyl.unibe.ch

The thalamic reticular nucleus (nucleus reticularis thalami, nRT) is a collection of inhibitory neurones organised into a thin layer separating the dorsal thalamus from the cortex (Scheibel & Scheibel, 1966; Houser *et al.* 1980). Three major synaptic inputs modulate the electrical response of these cells: excitatory inputs arising from layer VI cortical pyramidal cells (Bourassa *et al.* 1995) and thalamic relay cells (Harris, 1987) and carried by cortico-thalamic and thalamocortical fibre collaterals, and intra-nRT connections through chemical (Shu & McCormick, 2002) as well as, at least in rodents, electrical synapses (Landisman *et al.* 2002). In addition, other afferents reach the nRT from several sources and various modulators contribute non-specific effects to the membrane voltage of these cells (for review, see McCormick, 1992). NRT neurones in turn innervate those thalamic nuclei from which they receive input (Ohara & Lieberman, 1985; Crabtree, 1996; Cox *et al.* 1997; Wang *et al.* 2001), thus forming an intrathalamic disynaptic circuit which is linked to the cortex. However, they do not project directly to cortical areas (Scheibel & Scheibel, 1966; Jones, 1975).

The presence of a voltage-dependent low-threshold Ca^{2+} current (I_T) in thalamocortical cells and nRT neurones forms the electrophysiological basis for the two modes of action potential (AP) generation that these cells possess (Jahnsen & Llinás, 1984; Mulle *et al.* 1986; Avanzini *et al.* 1989). At hyperpolarised potentials, a sufficiently fast and large depolarising current can lead a thalamic cell to fire in bursts, while at more depolarised potentials, tonic discharges are prevalent. The burst firing mode is associated with periods of drowsiness or slow-wave sleep while tonic firing has been observed principally during states of wakefulness (Steriade & Llinás, 1988; Steriade *et al.* 1993; Sherman & Guillery, 1996). Interactions between nRT neurones and thalamocortical relay cells are responsible for the generation of spindle waves during sleep onset and are involved in certain forms of epilepsy (Steriade *et al.* 1993). In contrast, during tonic mode, the nRT is thought to be involved in attentional mechanisms in the awake animal (Crick, 1984; Weese *et al.* 1999). Thus, this nucleus may play a dual role dependent on the overall state of consciousness.

In rodents, the ventroposterior medial (VPm) and lateral (VPl) nuclei form a complex (ventrobasal complex, VB) of first-order relay cells that convey somatosensory information from lemniscal afferents to cortical area S1. Whether this information is simply passed on to the cortex without disruption of its content, or is significantly modulated by the thalamus is a major focus of recent research (Ahissar & Zacksenhouse, 2001; for reviews, see Sherman & Guillery, 1996; Nicolelis & Fanselow, 2002). Considering that thalamocortical axons of VB cells also innervate the nRT, an important question arises: is the message delivered to the nRT the same as the message

delivered to the cortex? Sherman & Guillery (1998) argue that synaptic connections can be divided into two sets: 'drivers', which reliably pass on a message to their postsynaptic targets, and 'modulators' whose actions are more subtle and rely on achieving a postsynaptic modification of the 'readiness' of a cell to respond to a driver input. In other words, can the synaptic connections made by VB cells onto nRT neurones be classified as 'drivers', 'modulators' or a mixture of both? Each answer can lead to a different view of the function of the nRT. The knowledge of the nature of the synaptic connections made by VB relay cells onto nRT neurones is therefore essential in understanding the role of the nRT.

Similarly, the synaptic outputs of the nRT play a crucial role in understanding its function. They include intra-nRT inhibitory pathways (Shu & McCormick, 2002), feedback inhibitory connections to thalamic relay cells (Cox *et al.* 1997) and a recently discovered pathway leading to higher-order thalamic nuclei (Crabtree *et al.* 1998). In rodents, the feedback pathway to the somatosensory thalamus is of particular interest, since it provides the main inhibitory source to thalamic relay cells (Barbaresi *et al.* 1986), due to the lack of local interneurones. Cox and colleagues (1997) have shown that nRT to VB synaptic connections can be strong and reliable when relayed by compact axonal arborisations of nRT neurones within the ventrobasal thalamus. Whether this inhibitory feedback drive to VB cells involves reciprocal disynaptic connections or acts mainly as a lateral suppressor of activity remains to be determined (Shosaku, 1986, Varga *et al.* 2002).

METHODS

Preparation

Juvenile (P14–20) Wistar rats were decapitated using a small animal guillotine according to our local Animal Care Committee guidelines (Service Vétérinaire: Office de l'agriculture du canton de Berne). Horizontal slices (300–350 μm thick) of the thalamus that included the nucleus reticularis (Fig. 1*A*) were prepared in an ice-cold sucrose-based solution equilibrated with 95 % O_2–5 % CO_2 (Huguenard & Prince, 1994). The slices were then transferred to an incubating bath chamber containing standard artificial cerebrospinal fluid (ACSF, equilibrated with 95 % O_2–5 % CO_2) maintained at 35 °C for 1 h prior to recording. The slicing solution contained (mM): 234 sucrose, 2.5 KCl, 1.25 NaH_2PO_4, 10 $MgCl_2$, 0.5 $CaCl_2$, 26 $NaHCO_3$, 11 glucose. The standard ACSF solution contained (mM): 125 NaCl, 2.5 KCl, 1.25 $NaHPO_4$, 1 $MgCl_2$, 2 $CaCl_2$, 25 $NaHCO_3$ and 10 glucose. The ACSF solution was also used during continuous superfusion of the recording chamber. In some experiments, 6,7-dinitroquinoxaline-2,3-dione (DNQX, 20 μM; Sigma), D-2-amino-5-phosphonopentanoic acid (D-AP5, 50 μM, Sigma) and/or bicuculline methiodide (BMI, 20 μM; Tocris Neuramin, Bristol, UK) were added to the superfusate.

Identification of thalamic relay cells and neurones of the nucleus reticularis

Slices were viewed under an upright microscope (BX50WI, Olympus Optical Co., Tokyo Japan) fitted with × 4 Plan/0.10 NA and × 40 W/0.8 NA objectives. The thalamic reticular formation (nRT) was visualised at low magnification and identified as a dark curved band running from the hippocampus to the third ventricle (see Fig. 1*A*). The VB of the thalamus was identified as a semi-dark area caudal and medial to the nRT. A digital picture was taken at the end of most experiments to determine the distance between the synaptically connected cells under study. Their stereotaxic location was also roughly estimated and projected onto the same horizontal plane for the purpose of Fig. 1*B*.

Electrophysiological recordings

Whole-cell voltage recordings from pre- and postsynaptic neurones were made using patch pipettes (3–5 MΩ) pulled from thick borosilicate capillaries (Hilgenberg GmbH, Germany) and filled with (mM): 135 potassium gluconate, 5 NaCl, 1 $MgCl_2$, 10 Hepes and 5 glucose, pH adjusted to 7.3 with KOH. All recordings were made at 34–36 °C. Briefly, an nRT neurone was initially patched, then the VB was 'scanned' using a searching pipette filled with regular intracellular solution to which a slight positive pressure was applied. The scanning began at the medial-most side of the VB, moving progressively towards the nRT until a response was observed in the nRT neurone, as a result of the depolarising effect of the high K^+ solution contained in our searching pipette. The searching pipette was subsequently removed and replaced with a clean pipette for intracellular patching of VB cells in the area where the response had been observed. Usually, 1–10 VB cells had to be tested before establishing a connection. The input resistance of the nRT cell was regularly monitored and remained stable throughout our recordings (95 ± 10 MΩ). Similarly, the series resistance was regularly monitored and compensated for, and remained below 20 MΩ in all our recordings (average 10 ± 1 MΩ). Once a synaptically connected pair of cells was obtained, single presynaptic action potentials (APs) were elicited by brief injection of a current pulse (duration 20–40 ms, amplitude 100–500 pA).

Membrane voltages were recorded with two Axoclamp-2B amplifiers in bridge mode (Axon Instruments, Foster City, CA, USA), low-pass filtered at 1 kHz and digitised at 5–10 kHz with a Labmaster LM-12 A/D converter (Scientific Solutions, Solon, OH, USA) and stored on the hard disk for off-line analysis.

Data analysis

Analysis of recorded signals was performed using Axograph 4.6 (Axon Instruments). Ensemble average responses were obtained by averaging 5–100 traces. Individual traces were ignored if background spontaneous synaptic activity was too apparent or if an AP failure was observed. The EPSP (or IPSP) rise times were determined as the mean time to rise from 10 to 90 % of the peak amplitude. The latency was determined as the time interval between the peak of the presynaptic AP and the time at which the average EPSP (or IPSP) had reached 5 % of its peak amplitude. In our paired-pulse experiments, the size of the second EPSP was linearly compensated for depolarisation-induced changes in driving force using a simple ohmic relationship to determine the amount of paired-pulse depression.

The decaying phase of EPSPs recorded in the present study could be well fitted with one or two exponential functions. In the latter case, we measured the weighted decay time constant according to the following formula:

$$\tau_{av} = (A_1\tau_1 + A_2\tau_2)/(A_1 + A_2),$$

where A_1 and A_2 are the y intercepts of the first and second exponential functions with the $x = 0$ axis at the peak of the EPSP, and τ_1 and τ_2 are the first and second decay time constants.

Weighted decay time constants were used throughout this study for ease of comparison.

The coefficient of variation (CV = S.D./mean) of EPSP amplitudes (Fig. 2*B*) was corrected for baseline noise by subtracting the variance of the baseline noise (measured over a 10 ms period preceding the EPSP) from the variance of the EPSP peak amplitude (excluding failures). Unless stated otherwise, all data are presented as means ± S.E.M.

Table 1. Time course of EPSPs at the VB cell to nRT neurone connection

	Mean	S.E.M.	*n*
EPSP amplitude (mV)	7.43	1.53	22
Rise time (10–90%) (ms)	0.63	0.03	22
Decay time constant (ms)	15.12	0.91	21
CV at peak	0.15	0.02	11

RESULTS

Inhibitory neurones of the nRT were identified on the basis of their anatomical location (Fig. 1*A*) as well as their characteristic firing pattern (Mulle *et al.* 1986; Avanzini *et al.* 1989). Resting membrane potentials were more negative than −60 mV in all cases (−68.5 ± 1.5 mV). At such potentials T-currents are de-inactivated and nRT neurones fire in bursts, while at more depolarised potentials, they adopt a tonic mode of firing. In some instances, spontaneous bursts of APs could be observed (data not shown). Presynaptic VB relay cells were also identified on the basis of their anatomical location (Fig. 1*A*) and their firing pattern which was distinct from that of nRT neurones (Jahnsen & Llinás, 1984). The majority of VB cells were anatomically identified as belonging to the VPm. Once an nRT neurone had been patched and a potential 'hot spot' had been found with the searching procedure (see Methods), 1–10 VB cells had to be tested before establishing a synaptic connection.

The anatomical location of 13 pairs of cells was projected onto the same horizontal plane of a thalamus slice diagram (Fig. 1*B*). In nearly all cases, the angle made by the straight line connecting a pair and an imaginary curved line running lengthwise through the nRT was close to 90 deg, indicating that axon collaterals emanating from thalamocortical fibres do not extend very far into the nRT (Harris, 1987). In a couple of pairs where this angle was substantially different from 90 deg, we found no significant increase in the EPSP

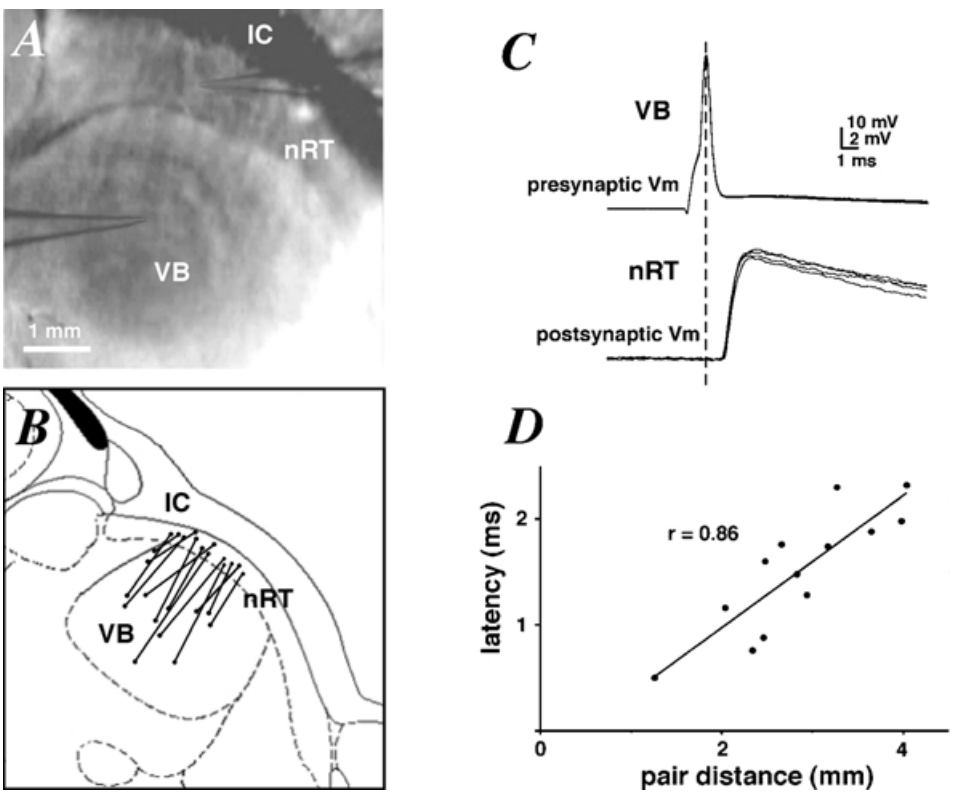

Figure 1. Correlation between latency and pair distance

A, photomicrograph of a horizontal thalamic slice, including pipette locations during paired recording. Scale bar = 1 mm. Abbreviations: nRT, nucleus reticularis thalami; IC, internal capsule; VB, ventrobasal complex. *B*, schematic diagram of the location of 13 synaptically coupled pairs of cells as in *A*. *C*, presynaptic APs (top traces) and unitary EPSPs (bottom traces) recorded from a synaptically coupled pair of cells as in *A*. *D*, plot of mean EPSP latencies against the distances between 13 pairs showing a strong positive correlation (Pearson's $r = 0.86$, $P < 0.001$). The inverse slope of the linear fit gives a propagation velocity of ~2 m s^{-1}.

latency. The direct distance between the somata of synaptically coupled VB–nRT cells ranged from 1.3 to 4 mm. Single presynaptic APs evoked by current injection into the soma of a VB cell elicited unitary EPSPs in the postsynaptic nRT neurone (Fig. 1*C*) with a latency that varied very little from trial-to-trial. The mean EPSP latency showed a positive correlation with distance in the 13 pairs for which a picture was taken (Fig. 1*D*; Pearson's $r = 0.86$, $P < 0.001$), giving a pre-to-postsynaptic transmission speed of ~2 m s^{-1}. Because synaptic delays are short (Sabatini & Regehr, 1999), this value corresponds roughly with the AP propagation speed in VB cells.

EPSP time course

An example of an average unitary EPSP is shown in Fig. 2*A*. Table 1 summarises our results obtained from 22 paired recordings. Mean EPSP amplitudes (excluding failures) ranged from 0.7 to 27 mV (mean: 7.4 mV), while 10–90 % EPSP rise times were below 1 ms in all 22 pairs. The only correlation between any of the measured parameters of Table 1 was found between the CV at the peak and the mean EPSP amplitude (Pearson's $r = -0.79$, $P < 0.001$). Moreover, the plot of CV against mean EPSP amplitude was well fitted with a hyperbolic function (Fig. 2*B*), indicating that synaptic terminals at the VB to nRT connections approximate the independent and identical release sites model (Redman, 1990). Peak amplitude histograms were narrow and well fitted by a Gaussian function (Fig. 2*C*). The average CV across 11 pairs from which over 40 traces had been recorded was 0.15, indicating that synaptic connections between VB cells and nRT neurones exhibit low variability in the total number of postsynaptic receptors activated.

Latency of unitary EPSPs

Several factors may influence the variance of latency distributions: background noise (i.e. signal-to-noise ratio), channel stochasticity and variable activation of synaptic contacts which are spread over the dendritic tree and/or soma of a neurone (for review, see Sabatini & Regehr, 1999). Within a single connection between a VB cell and an nRT neurone, the latency histogram is very narrow and closely fitted by a Gaussian function (Fig. 2*D*). Across several connections, the mean S.D. of the latency was 0.06 ± 0.02 ms. Thus, unitary EPSPs in nRT neurones elicited by presynaptic APs in a VB cell show a remarkably low variability in latency compared to those found in pairs of L4 or L5 pyramidal cells (Markram *et al.* 1997; Feldmeyer & Sakmann, 2000) or spiny stellate cells to L2/3 pyramidal cells (Feldmeyer *et al.* 2002). To achieve such a high degree of temporal convergence, synaptic contacts might be distributed at electrotonically equidistant sites on the somatodendritic membrane of nRT neurones.

VB to nRT unitary EPSP pharmacology

To estimate the relative contribution of NMDA receptor (NMDAR) and non-NMDAR to the total voltage of the EPSPs, we recorded unitary EPSPs in the presence of the NMDAR antagonist D-AP5 (50 μM) or in the presence of the AMPA receptor (AMPAR) antagonist DNQX (20 μM). EPSPs were measured either at potentials more negative than −70 mV or more positive than −60 mV, in order to determine whether a voltage dependence to the relative contributions of both types of receptors existed. At the end of some experiments, D-AP5 and DNQX were added to determine whether the EPSPs were completely glutamatergic; in all cases, a complete block was achieved. Figure 3*A* shows example traces of an EPSP recorded in control, D-AP5, DNQX or in both D-AP5 and DNQX. In D-AP5, the decay of the EPSP was accelerated while in DNQX, a slowly rising and decaying component remained, thus indicating a significant NMDAR-mediated component at rest.

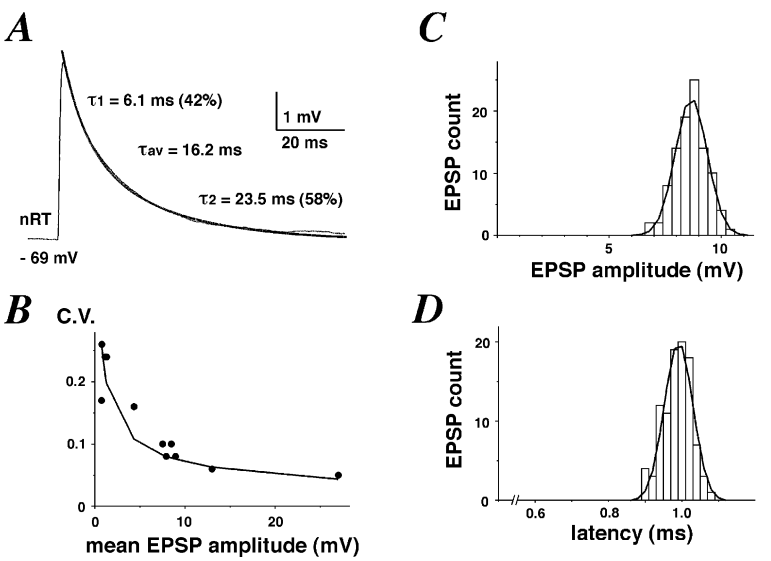

Figure 2. Latency and peak CV of unitary EPSPs

A, example average EPSP trace from a synaptic connection between a VB cell and nRT neurone. The decay phase was fitted with two exponential functions with time constants 6.1 and 23.5 ms, respectively. Their relative contribution to the total decay was 42 and 58 %, respectively. The weighted decay time constant is given as τ_{av}. *B*, plot of CV against the mean EPSP amplitude observed in 11 pairs, showing a strong negative correlation (Pearson's $r = -0.79$, $P < 0.001$). A hyperbolic fit ($CV = a/\sqrt{(\text{mean EPSP})}$) is overlaid. *C*, peak distribution of unitary EPSPs from a synaptic connection, fitted with a Gaussian function ($\sigma = 1.4$ mV). *D*, latency distribution of unitary EPSPs from a synaptic connection, fitted with a Gaussian function ($\sigma = 0.04$ ms). Note the narrowness of the distribution.

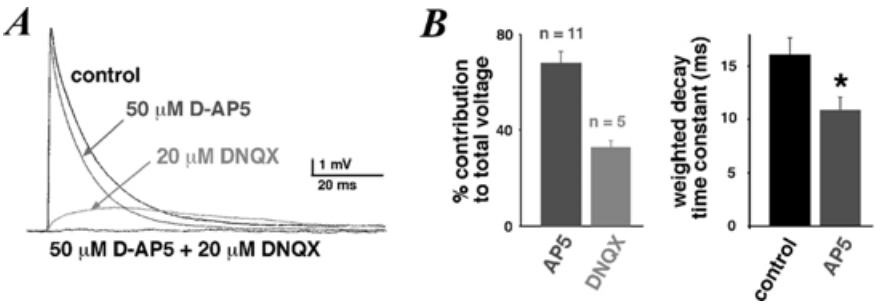

Figure 3. NMDA and non-NMDA components of unitary EPSPs

A, average EPSPs recorded in a cell in control, 50 μM D-AP5 and/or 20 μM DNQX. The holding potential was −60 mV. *B*, percentage contribution to the total integrated control voltage of residual EPSPs after perfusion of 50 μM D-AP5 or 20 μM DNQX integrated over 100 ms after onset. Mean weighted decay time constant of average EPSPs in control and 50 μM D-AP5 ($n = 5$, the difference between the two groups was significant, unpaired t test, $P < 0.05$).

In the presence of D-AP5, the EPSP voltage integrated over its entire time course was 68.1 ± 4.9 % ($n = 11$) of the integrated control voltage (Fig. 3*B*). In the presence of DNQX, the EPSP voltage was 32.8 ± 2.7 % ($n = 5$) of the control voltage. When EPSPs were measured at potentials more negative than −70 mV, the relative contributions became 71.4 ± 4.1 % ($n = 7$) and 30.5 ± 4.2 % ($n = 3$), respectively. When EPSPs were measured at potentials more positive than −60 mV, the relative contributions were 58.8 ± 9.8 % ($n = 5$) and 36.7 ± 0.8 % ($n = 3$), respectively (not shown). Thus, there is a small voltage dependence of both receptors' relative contributions in favour of the NMDAR at more depolarised potentials. More importantly, the NMDAR contribution did not suffer from a significant Mg^{2+}-dependent voltage block at potentials more negative than −70 mV (see Discussion).

Furthermore, we measured the effects of NMDAR block on the time course of the EPSPs. The average weighted decay time constant of the EPSPs fell from 16.0 ± 1.7 ms in control to 10.9 ± 1.2 ms ($n = 11$) in the presence of D-AP5 (Fig. 3*B*).

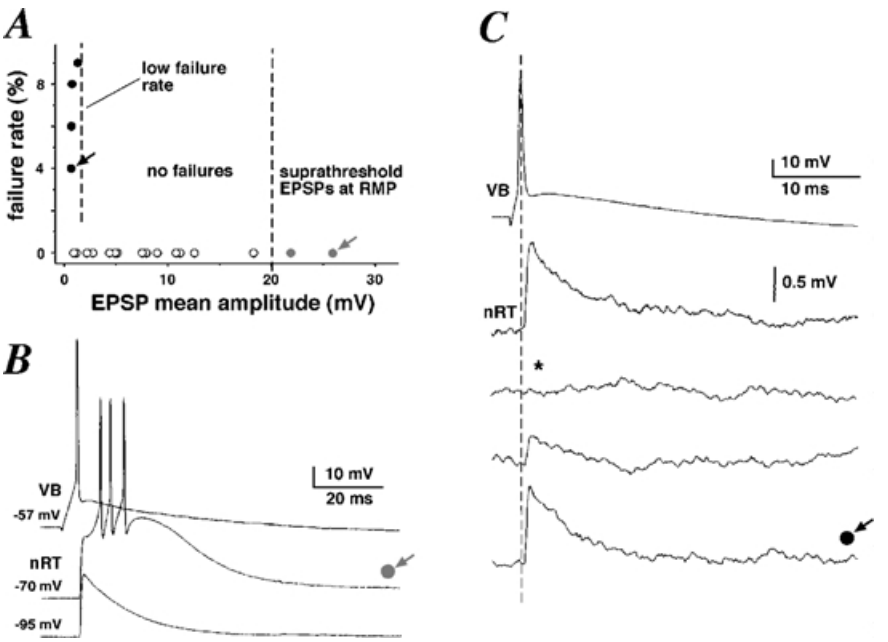

Figure 4. Unitary EPSPs fall into three categories

A, plot of failure rate against mean EPSP amplitude recorded for each pair, showing that 18 out of 22 pairs did not exhibit any transmission failure. *B*, example traces of a presynaptic action potential (AP; top trace) eliciting a suprathreshold unitary EPSP (middle trace) from a resting membrane potential of −70 mV. Hyperpolarisation of the nRT cell led to a subthreshold unitary EPSP (bottom trace). *C*, example traces of a presynaptic AP (top trace) eliciting small unitary EPSPs (bottom traces). * Example trace of a transmission failure.

Reliability of synaptic transmission

Synaptic transmission between VB cells and nRT neurones is very reliable (Fig. 4). Only four out of the 22 pairs we recorded from showed any amount of failure, and none showed a failure rate over 10 % (Fig. 4*A* and *C*). The average EPSP amplitude for those four connections was 0.86 ± 0.15 mV.

In two pairs, presynaptic APs elicited EPSPs in the nRT neurone that were suprathreshold at a resting membrane potential of −70 mV (Fig. 4*B*). Moreover, one evoked presynaptic AP could elicit a burst of APs in the nRT neurone, due to activation of a low-threshold calcium current. This burst of APs was always riding on a calcium spike (Fig. 4*B*). Injection of hyperpolarising current into the nRT neurone was necessary to elicit unitary subthreshold EPSPs (Fig. 4*B*). Moreover, insufficient hyperpolarisation could lead to EPSPs that were subthreshold, yet distorted by a large calcium spike (data not shown, $n = 4$). In all cases, only those EPSPs that were not distorted by I_T were selected for averaging. Since the resulting hyperpolarisation changed the driving force for sodium significantly, EPSP amplitudes were linearly scaled to their theoretical values at −70 mV.

Paired-pulse depression at VB to nRT synaptic connections

Short-term synaptic plasticity is a common feature of central and peripheral synapses (Zucker, 1989; Thomson, 2000*a*). Here, we investigated whether paired-pulse stimuli at reliable VB to nRT synapses led to short-term facilitation or depression.

Series of paired EPSPs with increasing interpulse intervals (from 5 to 40 ms, 5 ms increments) were recorded in four cells. At least five EPSPs were recorded, averaged and normalised at the peak of the first EPSP for each interpulse interval (Fig. 5*A*). Average EPSPs riding on top of the first EPSP were further corrected by subtraction and linear ohmic regression, assuming a reversal potential of 0 mV (Fig. 5*B*). A plot of the ratio of the 2nd peak/1st peak against the interpulse interval (Fig. 5*C*) revealed maximal depression at the shorter intervals. Depression was still apparent at the largest interval (29 ± 9 %, $n = 4$). There was no correlation between the amplitude of the first EPSP and the amount of depression ($P > 0.05$).

We further investigated the effects of short-term depression on the EPSP response to a burst of presynaptic APs. Hyperpolarising DC current injection into the VB cell allowed for a burst of 3 to 5 APs (frequency: 270 ± 30 Hz) to be evoked by a short depolarising intracellular current pulse. The summed EPSP response was maximal at the third or fourth successive EPSP (Fig. 5*D*). The ratio of the maximal summed EPSP peak to the first EPSP peak was 1.76 ± 0.17 ($n = 6$, e.g. Fig. 5*D*) when the maximal peak was observed on the third successive EPSP, or 2.01 ($n = 1$) when the maximal peak was observed on the fourth

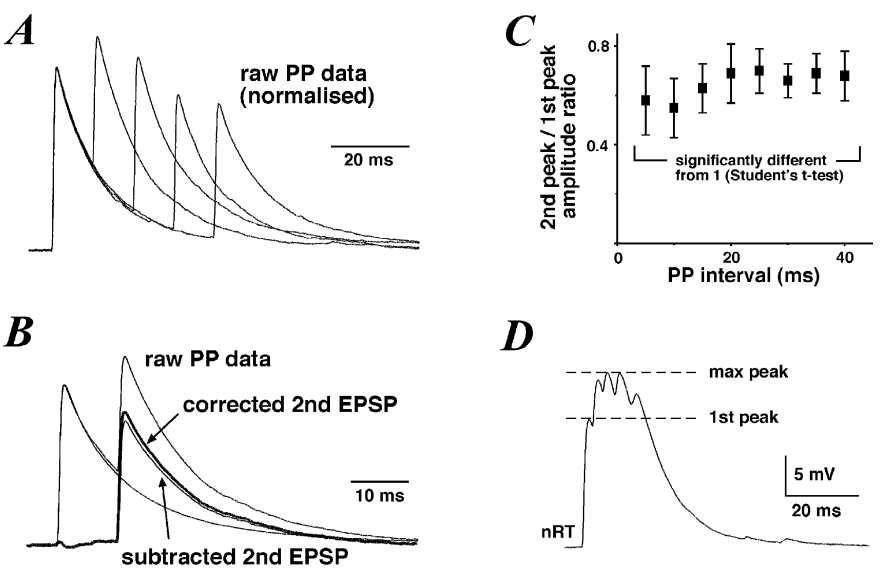

Figure 5. Paired-pulse depression at VB to nRT connections

A, example traces of paired-pulse (PP) data normalised at the peak of the first EPSP. Each trace is the average of 5 paired EPSPs. *B*, example PP trace illustrating the method employed for estimating the 2nd peak/1st peak ratio. Single EPSP traces were subtracted from PP data and the resulting EPSP traces were corrected for a decrease in driving force by linear extrapolation of the amplitude back to resting voltage. *C*, plot of the 2nd peak/1st peak ratio against the PP interval, showing that PP depression persists for over 40 ms. *D*, example trace of a burst of EPSPs recorded in an nRT neurone in response to a burst of APs evoked in the presynaptic VB cell. The first EPSP peak and maximal burst peak are highlighted by a dashed line.

successive EPSP (not shown). Thus, successive EPSPs elicited by a burst of presynaptic APs sum up sublinearly but can still lead to a cumulative depolarisation of the nRT neurone.

Reciprocally connected VB–nRT pair

In one out of 14 pairs tested, a reciprocal connection was observed (Fig. 6). In this experiment, single presynaptic APs in the VB cell elicited unitary EPSPs in the postsynaptic nRT neurone (average peak amplitude: 7.53 mV, average latency: 0.72 ms, not shown) while single presynaptic APs in the nRT neurone evoked unitary IPSPs in the postsynaptic VB cell (at a resting membrane potential of −60 mV) with an average peak amplitude of 0.77 mV, an onset latency of 0.76 ms and an average half-width of 59.8 ms (Fig. 6*A*). In this particular connection, no transmission failure was observed in the more than 100 IPSPs that were recorded. IPSPs were completely abolished in the presence of 10 μM bicuculline (Fig. 6*B*), indicating that they were mediated by activation of ionotropic $GABA_A$ receptors. IPSPs recovered completely after a 10 min washout period (data not shown). The absence of any $GABA_B$ receptor component in the IPSP cannot be considered conclusive, since the lack of GTP in our pipette solution rendered the detection of metabotropic responses unlikely (Sodickson & Bean, 1996). The IPSP reversal potential was close to −90 mV (data not shown), within the range of previously estimated values in these cells (Huguenard & Prince, 1994; Ulrich & Huguenard, 1997).

Since nRT neurones are capable of two modes of AP generation, we were interested in studying the effects of nRT burst firing on the IPSP response in the VB cell. Burst firing was evoked in the nRT neurone by injection of hyperpolarising intracellular DC. Series of three APs within a time window of less than 20 ms elicited in the VB cell three consecutive IPSPs with an average combined peak amplitude that was 2.1 times greater than the average peak amplitude of a single IPSP evoked by one presynaptic AP, indicating sublinear summation (Fig. 6*C*). Similarly Cox and colleagues (1997) observed that successive IPSCs in VB cells elicited by bursts of APs in nRT neurones were not linearly cumulative.

DISCUSSION

In the present study, we performed dual whole-cell voltage recordings between pairs of synaptically coupled VB cells and nRT neurones in order to determine the electrophysiological properties of this important connection in thalamocortical circuitry.

The advantages of our procedural methods are twofold: the possibility of antidromically activating corticothalamic fibres is removed, and the time course of recorded signals is not distorted by the high access resistance and/or shunting leak observed during intracellular microelectrode recordings (Pongracz *et al.* 1991). Moreover, our procedural method allowed us to test the existence of reciprocal connections, which have been postulated, but have never been physiologically observed between these two thalamic nuclei (Shosaku, 1986).

Our data indicate that synaptic connections made by VB cells onto nRT neurones possess some remarkable features: (1) the latency distribution of unitary EPSPs was very narrow; (2) unitary EPSPs fluctuated little and had almost no transmission failures; (3) unitary EPSPs could be suprathreshold from resting membrane potentials (see Figs 2*B*, 2*D* and 4*B*). Furthermore, the contribution of NMDA receptors to the total voltage of unitary EPSPs shows relatively little voltage dependence, suggesting that thalamocortical synapses onto nRT neurones might possess a rare type of NMDAR. Finally, a subset of cells form closed disynaptic loops, indicating that nRT to VB inhibition is both reciprocal and lateral.

Strength of unitary EPSPs

In our study, the distribution of EPSP amplitudes was unimodal and narrow and the average peak EPSP amplitude observed across all pairs of synaptically coupled VB cells and nRT neurones was over 7 mV. However, it is probable that its true value is somewhat smaller, since we

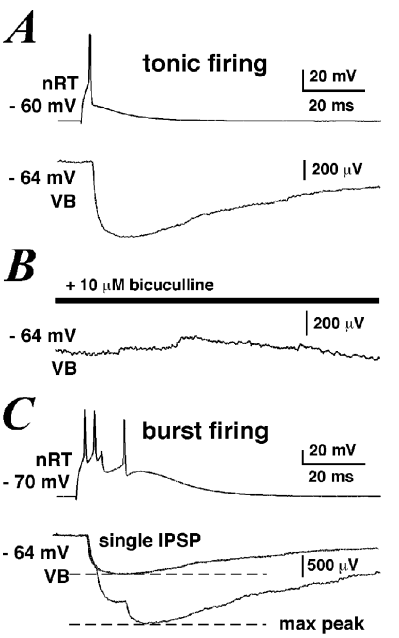

Figure 6. Unitary IPSPs recorded in a reciprocally connected VB–nRT pair

A, example trace of averaged IPSPs recorded in a VB cell (lower trace) elicited by a single presynaptic AP in an nRT neurone (top trace). *B*, IPSPs were abolished in the presence of 10 μM bicuculline. *C*, example trace of averaged IPSPs recorded in a VB cell (lower trace) elicited by a burst of presynaptic APs in an nRT neurone (top trace). The dashed lines indicate the locations at which peak amplitudes for single and triple IPSPs were measured.

were more likely to pick up larger EPSPs during our searching procedure (see Methods). Our findings indicate that unitary EPSPs from VB cells to nRT neurones can even be large enough to elicit APs in the postsynaptic cell from resting membrane potential. The size and release properties of the VB–nRT connections are quite unusual for central synapses (cf. Redman, 1990), but have been observed at thalamocortical synapses by stimulation of the thalamocortical fibres (see review by Castro-Alamancos & Connors, 1997). Such connections cannot be considered modulatory, and the existence of 'driver' inputs to the nRT has important consequences for thalamocortical circuitry (see later Discussion).

To rule out a contamination of EPSPs by low-threshold spikes (LTS), nRT neurones were always held below the activation threshold of I_T, which is ~−40 mV in these cells (Huguenard & Prince, 1992). In cases where an LTS was evoked by an EPSP (see Fig. 4*B*), the calcium spike was always clearly delayed, in agreement with the known slow onset kinetics of T-channels in nRT cells (Huguenard & Prince, 1992).

There was a negative correlation between peak CV and mean EPSP peak amplitude (Fig. 2*B*). However, peak CV was still relatively small and transmission failures few at weak connections, indicating that there was a high probability of release (*P*) at presynaptic terminals. This was confirmed by the occurrence of paired-pulse depression, a phenomenon associated with high *P* connections (Thomson, 2000*b*). We also found that EPSPs elicited by bursts of presynaptic APs summed sublinearly as previously described in perigeniculate neurones (PGN; Kim & McCormick, 1998). Thus, bursts of subthreshold EPSPs might not lead to significantly more depolarisation than a single EPSP elicited during tonic firing. However, during the occurrence of spindle waves, the simultaneous discharge of several VB cells converging onto a nRT would increase the safety factor to elicit APs in the postsynaptic cell from a hyperpolarised membrane potential (Kim & McCormick, 1998). It remains to be examined, however, whether a voltage-dependent amplification process that counteracts use-dependent EPSP depression, similar to that observed in layer 5 pyramidal neurones (Williams & Stuart, 1999), exists at depolarised potentials in nRT neurones.

Temporal precision of unitary EPSPs

Thalamocortical fibres are thicker than their cortico-thalamic counterparts but the collaterals they give off as they traverse the nRT appear to thin out and extend to a variable degree into the nRT (Harris, 1987). Since thicker axons conduct APs faster than thinner ones, the main delay observed between the initiation of an AP at the axon hillock of a relay cell and its spread into the presynaptic terminals of relay neurones might be due to the distance which those axon collaterals extend into the nRT. The minimal conduction velocity was found to be around 2 m s^{-1}, as would be expected for myelinated or partly myelinated axons (Sabatini & Regehr, 1999). Since VB cell axon collaterals can extend up to 350 μm into the nRT of adult rats (Harris, 1987), the maximum delay between the arrival of an AP at two separate nRT neurones contacted by such a collateral would be less than 0.2 ms.

Our findings indicate that the timing of the onset of EPSPs varied very little from trial-to-trial within a synaptic connection (see Fig. 2*D*). The synaptic contacts made by VB axons onto nRT neurones are typically found on proximal dendrites and contain several release sites (Liu, 1997). Since we did not observe an increase in EPSP rise time with average peak EPSP amplitude in our recordings, multiple release sites must be arranged in close proximity to each other (Sabatini & Regehr, 1999). This postsynaptic organisation, combined with fast axonal conduction velocity, adds to the observed temporal precision of the VB to nRT pathway.

NMDAR and non-NMDAR contributions to unitary EPSPs

The pharmacological profile of EPSPs recorded in the present study suggests that both NMDAR and non-NMDAR contribute substantially to the total voltage of EPSPs during regular synaptic transmission rate. The NMDAR-mediated component of EPSPs showed little sensitivity to voltage-dependent Mg^{2+}-block at resting membrane potentials, a feature associated with the presence of either the NR2C or NR2D subunit in heteromeric NMDAR-subtypes (Monyer *et al.* 1994; Kuner & Schoepfer, 1996; Momiyama *et al.* 1996; Vicini *et al.* 1998). Several regional distribution studies of NMDAR subunits point to the presence of NR2C and NR2D in the thalamus (Wenzel *et al.* 1996). However, no study has specifically investigated the presence of NR2C or NR2D subunits in the nucleus reticularis on a synaptic level and the precise subunit composition of NMDA receptors at this synapse remains to be determined. The relatively fast kinetics of the observed NMDAR-dependent response is likely to point towards an involvement of NR2C, in line with anatomical data (Wenzel *et al.* 1995). On the other hand, the distribution of AMPAR subunits in nRT neurones is known to the synaptic level. Thalamoreticular synapses arising from VB cells mainly contain GluR2/3 and GluR4 subunits (Liu *et al.* 1997; Mineff & Weinberg, 2000). Interestingly GluR4-rich AMPAR exhibit fast kinetics (Mosbacher *et al.* 1994), a property useful in pathways requiring precise temporal resolution (Trussell, 1999).

NMDA receptors have been shown to contribute to the generation of spindle-like oscillation in rat thalamic slices with intact intra-thalamic connectivity (Jacobsen *et al.*, 2001). Likewise, at lemnisco–thalamic synapses in relay cells, NMDARs have been shown to be effective at activating low-threshold calcium spikes in thalamic relay

cells (Turner *et al.* 1994). Our data support a role for NMDA receptors during regular excitatory synaptic transmission within the thalamic circuitry.

Implications for thalamocortical circuitry

The ventrobasal complex of the thalamus (which includes VPl and VPm) relays somatotopically organised somatosensory information from the contralateral body to the somatosensory cortex. Likewise, the nRT has been shown to be topographically organised in modality-specific sectors (Mitrofanis & Guillery, 1993). Due to the lack of interneurones in rodent VB (Barbaresi *et al.* 1986), the nRT is the only source of inhibitory input to relay cells. Whether the nRT acts mainly through lateral inhibition, recurrent feedback or both has important consequences for thalamic circuitry (e.g. Sherman & Koch, 1986). There is experimental evidence for lateral and feedback inhibition. Cross-correlation studies have shown that reciprocal VB–nRT connections exist in a subset of cells (Shosaku, 1986), while the occurrence of isolated IPSPs after stimulating sensory inputs indicates lateral inhibition (Brecht & Sakmann, 2002; Castro-Alamancos, 2002). In agreement, our study disclosed one mutually connected pair out of 14 tested (i.e. overall ~7 % of connections). Although our results might underestimate the actual percentage of reciprocal connections, due to severed connections in the slice, our data support the existence of recurrent as well as lateral inhibition in the nRT–VB projection. Anatomical findings in rat VPm show that nRT cells project to their homotopical barreloid (Desilets-Roy *et al.* 2002). Since dendrites of relay cells actually cross into neighbouring barreloids, this would allow for lateral as well as reciprocal inhibition (Varga *et al.* 2002).

The strength and temporal precision of synaptic connections made by VB cells onto nRT neurones in this study is more surprising. Anatomical studies in the adult rat have shown that each thalamic barreloid may contain up to 300 neurones (Land *et al.* 1995), while there are only between 10 and 30 neurones in the nRT corresponding to the same vibrissa receptive field (Shosaku, 1986). Large unitary EPSPs would therefore not appear necessary in producing the large and fast depolarisation required to activate I_T and elicit burst firing in nRT neurones if several smaller EPSPs converge to the same cell (cf. Kim & McCormick, 1998). Here, we postulate that large unitary EPSPs might instead be involved in rapid lateral inhibition in the somatosensory thalamus in the awake animal while maintaining its 'readiness' to respond to further stimulation. Similarly, the short time course of IPSCs observed in thalamic relay cells (Cox *et al.* 1997) suggests that feedback inhibition from nRT neurones is also temporally restricted. Thus, nRT would control ongoing activity in the rat somatosensory thalamus on a short time scale, setting a brief 'window of opportunity' for cortical integration of sensory information. This point of view is supported by *in vivo* studies in relay cells showing an increase in the receptive field size and an enhancement of tonic *vs.* phasic responses after surgical or pharmacological disinhibition (Lee *et al.* 1994; Hartings & Simons, 2000). Thus, the 'searchlight' would serve to enhance contrast in the temporal and spatial domain.

REFERENCES

Ahissar E & Zacksenhouse M (2001). Temporal and spatial coding in the rat vibrissal system. *Prog Brain Res* **130**, 75–87.

Avanzini G, de Curtis M, Panzica F & Spreafico R (1989). Intrinsic properties of nucleus reticularis thalami neurones of the rat studied *in vitro*. *J Physiol* **416**, 111–122.

Barbaresi P, Spreafico R, Frassoni C & Rustioni A (1986). GABAergic neurons are present in the dorsal column nuclei but not in the ventroposterior complex of rats. *Brain Res* **382**, 305–326.

Bourassa J, Pinault D & Deschênes M (1995). Corticothalamic projections from the cortical barrel field to the somatosensory thalamus in rats: a single-fibre study using biocytin as an anterograde tracer. *Eur J Neurosci* **7**, 19–30.

Brecht M & Sakmann B (2002). Whisker maps of neuronal subclasses of the rat ventral posterior medial thalamus, identified by whole-cell voltage recording and morphological reconstruction. *J Physiol* **538**, 495–515.

Castro-Alamancos MA (2002). Different temporal processing of sensory inputs in the rat thalamus during quiescent and information processing states *in vivo*. *J Physiol* **539**, 567–578.

Castro-Alamancos MA & Connors BW (1997). Thalamocortical synapses. *Prog Neurobiol* **51**, 581–606.

Cox CL, Huguenard JR & Prince DA (1997). Nucleus reticularis neurons mediate diverse inhibitory effects in thalamus. *Proc Natl Acad Sci U S A* **94**, 8854–8859.

Crabtree JW (1996). Organization in the somatosensory sector of the cat's thalamic reticular nucleus. *J Comp Neurol* **366**, 207–222.

Crabtree JW, Collingridge GL & Isaac JTR (1998). A new intrathalamic pathway linking modality-related nuclei in the dorsal thalamus. *Nat Neurosci* **1**, 389–394.

Crick F (1984). Function of the thalamic reticular complex: the searchlight hypothesis. *Proc Natl Acad Sci U S A* **81**, 4586–4590.

Desilets-Roy B, Varga C, Lavallee P & Deschênes M (2002). Substrate for cross-talk inhibition between thalamic barreloids. *J Neurosci* **22**, RC218.

Feldmeyer D, Lubke J, Silver RA & Sakmann B (2002). Synaptic connections between layer 4 spiny neurone-layer 2/3 pyramidal cell pairs in juvenile rat barrel cortex: physiology and anatomy of interlaminar signalling within a cortical column. *J Physiol* **538**, 803–822.

Feldmeyer D & Sakmann B (2000). Synaptic efficacy and reliability of excitatory connections between the principal neurones of the input (layer 4) and output layer (layer 5) of the neocortex. *J Physiol* **525**, 31–39.

Harris RM (1987). Axon collaterals in the thalamic reticular nucleus from thalamocortical neurons of the rat ventrobasal thalamus. *J Comp Neurol* **258**, 397–406.

Hartings JA & Simons DJ (2000). Inhibition suppresses transmission of tonic vibrissa-evoked activity in the rat ventrobasal thalamus. *J Neurosci* **20**, RC100 (1–5).

Houser CR, Vaughn JE, Barber RP & Roberts E (1980). GABA neurons are the major cell types of the nucleus reticularis thalami. *Brain Res* **416**, 187–191.

Huguenard JR & Prince DA (1992). A novel T-type current underlies prolonged Ca^{2+}-dependent burst firing in GABAergic neurons of rat thalamic reticular neurons. *J Neurosci* **12**, 3804–3817.

Huguenard JR & Prince DA (1994). Intrathalamic rythmicity studied *in vitro*: nominal T-current modulation causes robust antioscillatory effects. *J Neurosci* **14**, 5485–5502.

Jacobsen RB, Ulrich D & Huguenard JR (2001). GABA(B) and NMDA receptors contribute to spindle-like oscillations in rat thalamus *in vitro*. *J Neurophysiol* **86**, 1365–1375.

Jahnsen H & Llinás R (1984). Ionic basis for the electro-responsiveness and oscillatory properties of guinea-pig thalamic neurones *in vitro*. *J Physiol* **349**, 227–247.

Jones EG (1975). Some aspects of the organization of the thalamic reticular complex. *J Comp Neurol* **162**, 285–308.

Kim U & McCormick DA (1998). The functional influence of burst and tonic firing mode on synaptic interactions in the thalamus. *J Neurosci* **18**, 9500–9516.

Kuner T & Schoepfer R (1996). Multiple structural elements determine subunit specificity of Mg^{2+} block in NMDA receptor channels. *J Neurosci* **16**, 3549–3558.

Land PW, Buffer SA Jr & Yaskosky JD (1995). Barreloids in adult rat thalamus: three-dimensional architecture and relationship to somatosensory cortical barrels. *J Comp Neurol* **355**, 573–588.

Landisman CE, Long MA, Beierlein M, Deans MR, Paul DL & Connors BW (2002). Electrical synapses in the thalamic reticular nucleus. *J Neurosci* **22**, 1002–1009.

Lee SM, Friedberg MH & Ebner FF (1994). The role of GABA-mediated inhibition in the rat ventral posterior medial thalamus. I. Assessment of receptive field changes following thalamic reticular nucleus lesions. *J Neurophysiol* **71**, 1702–1715.

Liu X-B (1997). Subcellular distribution of AMPA and NMDA receptor subunit immunoreactivity in ventral posterior and reticular nuclei of rat and cat thalamus. *J Comp Neurol* **388**, 587–602.

Markram H, Lübke J, Frotscher M, Roth A & Sakmann B (1997). Physiology and anatomy of synaptic connections between thick-tufted pyramidal neurons in the developing rat neocortex. *J Physiol* **500**, 409–440.

McCormick DA (1992). Neurotransmitter actions in the thalamus and cerebral cortex and their role in neuromodulation of thalamocortical activity. *Prog Neurobiol* **39**, 337–388.

Mineff EM & Weinberg RJ (2000). Differential synaptic distribution of AMPA receptor subunits in the ventral posterior and reticular thalamic nuclei of the rat. *Neuroscience* **101**, 969–982.

Mitrofanis J & Guillery RW (1993). New views of the thalamic reticular nucleus in the adult and the developing brain. *Trends Neurosci* **16**, 240–245.

Momiyama A, Feldmeyer D & Cull-Candy SG (1996). Identification of a native low-conductance NMDA channel with reduced sensitivity to Mg^{2+} in rat central neurones. *J Physiol* **494**, 479–492.

Monyer H, Burnashev N, Laurie DJ, Sakmann B & Seeburg PH (1994). Developmental and regional expression in the rat brain and functional properties of four NMDA receptors. *Neuron* **12**, 529–540.

Mosbacher J, Schoepfer R, Monyer H, Burnashev N, Seeburg PH & Ruppersberg JP (1994). A molecular determinant for submillisecond desensitization in glutamate receptors. *Science* **266**, 1059–1062.

Mulle C, Madariaga A & Deschênes M (1986). Morphology and electrophysiological properties of reticularis thalami neurons in cat: *in vivo* study of a thalamic pacemaker. *J Neurosci* **6**, 2134–2145.

Nicolelis MA & Fanselow EE (2002). Thalamocortical optimization of tactile processing according to behavioral state. *Nat Neurosci* **5**, 517–523.

Ohara PT & Lieberman AR (1985). The thalamic reticular nucleus of the adult rat: experimental anatomical studies. *J Neurocytol* **14**, 365–411.

Pinault D & Deschênes M (1998). Anatomical evidence for a mechanism of lateral inhibition in the rat thalamus. *Eur J Neurosci* **10**, 3462–3469.

Pongracz F, Firestein S & Shepherd GM (1991). Electrotonic structure of olfactory sensory neurons analyzed by intracellular and whole cell patch techniques. *J Neurophysiol* **65**, 747–758.

Redman S (1990). Quantal analysis of synaptic potentials in neurons of the central nervous system. *Physiol Rev* **70**, 165–198.

Sabatini BL & Regehr WG (1999). Timing of synaptic transmission. *Annu Rev Physiol* **61**, 521–542.

Scheibel ME & Scheibel AB (1966). The organization of the nucleus reticularis thalami: a Golgi study. *Brain Res* **1**, 43–62.

Sherman SM & Guillery RW (1996). Functional organization of thalamocortical relays. *J Neurophysiol* **76**, 1367–1395.

Sherman SM & Guillery RW (1998). On the actions that one nerve cell can have on another: distinguishing 'drivers' from 'modulators'. *Proc Natl Acad Sci U S A* **95**, 7121–7126.

Sherman SM & Koch C (1986). The control of retinogeniculate transmission in the mammalian lateral geniculate nucleus. *Exp Brain Res* **63**, 1–20.

Shosaku A (1986). Cross-correlation analysis of a recurrent inhibitory circuit in the rat thalamus. *J Neurophysiol* **55**, 1030–1043.

Shu Y & McCormick DA (2002). Inhibitory interactions between ferret thalamic reticular neurons. *J Neurophysiol* **87**, 2571–2576.

Sodickson DL & Bean BP (1996). GABAB receptor-activated inwardly rectifying potassium current in dissociated hippocampal CA3 neurons. *J Neurosci* **16**, 6374–6385.

Steriade M & Llinás RR (1988). The functional states of the thalamus and the associated neuronal interplay. *Physiol Rev* **68**, 649–742.

Steriade M, McCormick DA & Sejnowski TJ (1993). Thalamocortical oscillations in the sleeping and aroused brain. *Science* **262**, 679–685.

Thomson AM (2000*a*). Molecular frequency filters at central synapses. *Prog Neurobiol* **62**, 159–196.

Thomson AM (2000*b*). Facilitation, augmentation and potentiation at central synapses. *Trends Neurosci* **23**, 305–312.

Trussell LO (1999). Synaptic mechanisms for coding timing in auditory neurons. *Annu Rev Physiol* **61**, 477–496.

Turner JP, Leresche N, Guyon A, Soltesz I & Crunelli V (1994). Sensory input and burst firing output of rat and cat thalamocortical cells: the role of NMDA and non-NMDA receptors. *J Physiol* **480**, 281–295.

Ulrich D & Huguenard JR (1997). Nucleus-specific chloride homeostasis in rat thalamus. *J Neurosci* **17**, 2348–2354.

Varga C, Sik A, Lavallée P & Deschênes M (2002). Dendroarchitecture of relay cells in thalamic barreloids: a substrate for cross-whisker modulation. *J Neurosci* **22**, 6186–6194.

Vicini S, Wang JF, Li JH, Zhu WJ, Wang YH, Luo JH, Wolfe BB & Grayson DR (1998). Functional and pharmacological differences between recombinant *N*-methyl-D-aspartate receptors. *J Neurophysiol* **79**, 555–566.

Wang S, Bickford ME, Van Horn SC, Erisir A, Godwin DW & Sherman SM (2001). Synaptic targets of thalamic reticular nucleus terminals in the visual thalamus of the cat. *J Comp Neurol* **440**, 321–341.

Weese GD, Phillips JM & Brown VJ (1999). Attentional orienting is impaired by unilateral lesions of the thalamic reticular nucleus in the rat. *J Neurosci* **19**, 10135–10139.

Wenzel A, Scheurer L, Kunzi R, Fritschy JM, Mohler H & Benke D (1995). Distribution of NMDA receptor subunit proteins NR2A, 2B, 2C and 2D in rat brain. *Neuroreport* **29**, 45–48.

Wenzel A, Villa M, Mohler H & Benke D (1996). Developmental and regional expression of NMDA receptor subtypes containing the NR2D subunit in rat brain. *J Neurochem* **66**, 1240–1248.

Williams SR & Stuart GJ (1999). Mechanisms and consequences of action potential burst firing in rat neocortical pyramidal neurons. *J Physiol* **521**, 467–482.

Zucker RS (1989). Short-term synaptic plasticity. *Annu Rev Neurosci* **12**, 13–31.

Acknowledgements

This work was supported by Swiss National Foundation grant no. 31-58961.99.